

Aggregation and weak gel formation by pectic polysaccharide homogalacturonan

Piotr Mariusz Pieczywek ^{a,*}, Jolanta Cieśla ^a, Wojciech Płaziński ^b, Artur Zdunek ^a

^a Institute of Agrophysics, Polish Academy of Sciences, Doświadczalna 4, 20-270 Lublin, Poland

^b Jerzy Haber Institute of Catalysis and Surface Chemistry, Polish Academy of Sciences, Niezapominajek 8, Cracow, 30-239, Poland



ARTICLE INFO

Keywords:

Pectin
Homogalacturonan
Self-assembly
Dissipative particle dynamics
Networking
Gelation

ABSTRACT

This study presents a novel model of homogalacturonan (HG) based on the dissipative particle dynamics (DPD). The model was applied to investigate the mechanism of self-aggregation of low-methoxylated homogalacturonan in aqueous solutions in the absence of cations. The coarse-grained model provided new insights into the structural features of HG aggregates and networks in aqueous solutions. Depending on the properties and concentration of polysaccharides, two major patterns of self-assembly were observed for HG - ellipsoidal aggregates and a continuous three-dimensional network. Simulations showed that a decrease in the degree of dissociation of HG results in a higher rate of self-aggregation, as well as facilitating the formation of larger assemblies or thicker nanofilaments depending on the type of final self-assembly. Simulations of polysaccharides of different chain lengths suggested the existence of a structural threshold for the formation of a spatial network for HG consisting of less than 35 GalA units.

1. Introduction

Pectins are recognized as an essential element of plant cell walls and as a group of chemical compounds commonly used as gelling substances (Thakur, Singh, Handa & Rao, 1997; Pérez, Rodríguez-Carvajal, & Doco, 2003; Palin & Geitmann, 2012). However, due to their inherent complexity, these compounds still elude a full functional and structural description. The major difficulty arises from the fact that the structure of pectin varies according to the source (plant), tissue type, developmental and metabolic stage and conditions of extraction (Round, Rigby, Mac-Dougall, & Morris, 2010; Billy et al., 2008; Li et al., 2020). Despite the differences in perception of the macro-scale assemblies formed by pectin as well as their mutual interactions with other polysaccharides, researchers are certain that the molecular structure of pectin is a key factor in shaping its functional features (Cosgrove & Anderson, 2020; Broxterman & Schols, 2018).

In the commonly accepted nomenclature, pectins are compounds containing at least 65 % galacturonic acid (GalA). When galacturonic acid combines with other sugars it forms five major structural groups of pectic polysaccharides including homogalacturonan (HG), xylogalacturonan (XGA), apiogalacturonan (AGA), rhamnogalacturonan I (RG-I), rhamnogalacturonan II (RG-II) (Caffall & Mohnen, 2009). Among

these, HG is a polymer of α -1,4-linked D-galacturonic acid that can account for more than 60 % of the pectin present in the plant cell wall (Ridley, O'Neill, & Mohnen, 2001). Studies have shown that higher amounts of HG in plants correlate with an increase in plant cell wall stiffness (Person et al., 2007; Ralet et al., 2008). A positive correlation of HG with cellular adhesion was also observed (Bouton et al., 2002; Mouille et al., 2007).

The unique properties of HG have been attributed to its molecular structure. The carboxyl groups of the HG galacturonate units may be methyl-esterified to a degree and in a pattern which is regulated during plant development (Wolf, Mouille, & Pelloux, 2009). Most importantly, the degree of methylation (DM) of the pectin influences its network formation capabilities and ability to form higher-order structures (Grant, Morris, Rees, Smith, & Thom, 1973; Oakenfull, 1991). The number and distribution of methyl-esterified carboxylic groups are regulated during plant development (Wolf et al., 2009). Pectin with a DM of less than 50 % (low-methoxyl pectin – LM) forms a gel in the presence of a crosslinking agent such as Ca^{2+} and within a pH range of 2–6 (Thibault & Ralet, 2003). However, there are some studies showing that LM pectin gelation is not limited to acidic media or to the presence of calcium ions (Gawkowska, Cieśla, Zdunek, & Cybulska, 2019; Gilsenan, Richardson, & Morris, 2000; Ström, Schuster, & Goh, 2014; Yang

* Corresponding author.

E-mail address: p.pieczywek@ipan.lublin.pl (P.M. Pieczywek).

et al., 2018).

Peaucelle, Wightman, and Hofte (2015) demonstrated *in vivo* that demethylated HG and the resulting negatively charged acidic carboxyl groups are present in rapidly expanding cells, and that demethylation correlates with wall elasticity change. Later, Haas, Wightman, Meyerowitz, and Peaucelle (2020) reported that in the anticlinal walls of pavement cells of *Arabidopsis* (*Arabidopsis Thalina*) pectin HG assembles into discrete filaments. It has been suggested that demethylation causes the HG nanofilament to locally expand in a radial direction leading to cell wall expansion. This unorthodox structural image of plant cell wall polysaccharides was supported by data obtained using 3D direct stochastic optical reconstruction microscopy (3D-dSTORM). However, previous studies based on chemical analysis, as well as on the direct imaging of the molecular structure of pectin using AFM, did not confirm the presence of such structures (Paniagua et al., 2017; Pieczywek, Koziol, Plaziński, Cybulski, & Zdunek, 2020; Posé, Kirby, Mercado, Morris, & Quesada, 2012; Zdunek, Koziol, Pieczywek, & Cybulski, 2014).

In this regard, numerical methods may be a useful tool to enable the study of the properties of higher-order structures formed by homogalacturonan. To date, numerical simulations of pectic polysaccharides have included studies of the conformational stability of galacturonic acid oligomers and their configurational features in aqueous solutions (Cros, Garnier, Axelos, Imbert, & Pérez, 1996; Manunza, Deiana, Pintore, & Gessa, 1997; Noto, Martorana, Bulone, & San Biagio, 2005; Panczyk, Gaweda, Drach, & Plazinski, 2018), interactions with calcium ions (Manunza, Deiana, Pintore, & Gessa, 1997; Braccini & Pérez, 2001; Panczyk et al., 2018) or interactions with other pectic polysaccharides (Makshakova, Gorshkova, Mikshina, Zuev, & Perez, 2017). These studies were carried out using molecular modelling or molecular dynamics simulations which provide an atom-by-atom model of molecular interactions in the most comprehensive way possible at present, however, this only applies to a limited size of structure and relatively short timescales. In recent times, a stochastic mesoscale particle model based on a dissipative particle dynamics (DPD) force field was introduced to study large-scale assemblies of homogalacturonan in water solutions (Pieczywek, Plaziński, & Zdunek, 2020). The model was capable of simulating GalA units at different degrees of protonation of the carboxyl group. A study demonstrated the successful application of the proposed parametrization method which allowed for the reproduction of the structural and transport properties of the target system.

The current study further explores the previously calibrated DPD force field to investigate the mechanism of LM homogalacturonan self-aggregation in the absence of metal cations. The model of homogalacturonan was used to simulate the effects of chain length, galacturonic acid concentration and the different protonation degrees of carboxyl groups on self-assembly mechanisms in aqueous solutions. The coarse-grained modelling approach provided new insights into the structural features of HG aggregates and networks in water, and produced the first large-scale simulations of aqueous homogalacturonan solutions. The numerical study was supported by the initial laboratory tests of GalA aqueous solutions which provided evidence of the qualitative relationship between the mutual interactions of GalA units and the size of associates at different concentrations and pH.

2. Materials and methods

2.1. Sample preparation

A series of aqueous solutions with the D-galacturonic acid (GalA; Sigma Aldrich, Poznan, Poland) concentration ranging from 10^{-5} to $2 \cdot 10^{-1}$ M was prepared using ultrapure MilliQ water.

In order to investigate the influence of the dissociation degree (α) of GalA molecules on the association process, the pH of the GalA solutions at concentrations of $3.0 \cdot 10^{-3}$, $3.3 \cdot 10^{-2}$ and $2.0 \cdot 10^{-1}$ M were adjusted to 0.35 ± 0.03 ($\alpha = 0.00$), 3.51 ± 0.04 ($\alpha = 0.50$) and 10.48 ± 0.16 ($\alpha =$

1.00) by the adding 1 M HCl or 1 M NaOH. The ionic strength of the solutions was adjusted to 3 M using KCl. The value of pH corresponding to the appropriate α at 20°C was estimated using the pK_a value of 3.51 ± 0.01 and the Henderson-Hasselbalch equation (Kohn & Kováč, 1978).

An Oakton pH Spear Waterproof Pocket Tester (Cole-Parmer, Vernon Hills, Illinois, US) was used for pH determination (3 repetitions). Before further investigation all solutions were gently mixed for 24 hours at 20°C .

2.2. Determination of particle size distribution and electrophoretic mobility

A Dynamic Light Scattering (DLS) method with a non-invasive back scattering technique (173° detection angle) was used to obtain the particle size (hydrodynamic diameter) distributions for the samples studied (ISO 22412, 2017; Zetasizer Nano User Manual et al., 2004). It was assumed that the presence of clusters of GalA molecules are the source of local differences in optical properties between these associates and the bulk solution, this affects light scattering. The size of the GalA associates was expressed in terms of a median radius calculated from the particle-size distribution.

Electrophoretic mobility (EM) was measured using Laser Doppler Electrophoresis (LDE) (Mayinger, 1994) and the electrokinetic (zeta) potential (ZP) values were calculated automatically with apparatus software using Henry's equation (Delgado, Gonzales-Caballero, Hunter, Koopal, & Lyklema, 2007). Electrolytic conductivity (EC) was determined simultaneously with EM. The measurements were performed using Zetasizer Nano ZS apparatus (Malvern Ltd., Malvern, UK) in 3 repetitions at 20°C . Statistical analyses (Anova/Manova, Statistica 13, StatSoft Poland Ltd., Cracow, Poland) were performed for the EM and ZP results obtained for different systems tested.

2.3. Dissipative particle dynamics simulations

The structures presented in this study were obtained using coarse-grained representations of the target systems – homogalacturonan chains in water solutions – which were simulated using dissipative particle dynamics (DPD). An extensive overview of the dissipative particle dynamics simulation method has been provided by Moeendarbary, Ng, and Zangeneh (2009) and Groot and Rabone (2011). Detailed formulations of the DPD method are also provided in Supplementary Information. DPD coarse-grained particles represent clusters of atoms called beads, which interact with the neighbouring beads via three basic non-bonded interaction forces, a conservative force \vec{F}_{ij}^C , a dissipative force \vec{F}_{ij}^D and a random force \vec{F}_{ij}^R . These forces can act within a specific length range, called the cut-off radius r_c . In this study, the standard DPD force field based on the data extracted from a united-atom molecular dynamics was applied to reproduce the structural and transport properties (diffusivity) of polysaccharide chains as well as their mutual interactions and interactions with the environment (water molecules). The CG level assumed that one DPD bead corresponds to a single unit of galacturonic acid (or four water molecules), and that it is represented by spherical force potential, negating any steric effects. In order to simulate polysaccharide molecular chains, the adjacent beads were constrained with permanent lengths and angular bonds, which are described using harmonic spring quadratic potentials. Dissipative particle dynamics were applied to study the effect of the dissociation degree of carboxyl groups of galacturonic acid on the gelation of pectin in water solutions. The galacturonic acid units were simulated in two states of the protonation of carboxyl groups – protonated/undissociated (GalA) and deprotonated/dissociated (GalA(-)). The full set of force field parameters and simulation settings are described in Supplementary Information. For a complete description of the model definition and parametrization scheme readers are referred to a recently published

paper by Pieczywek, Płaziński et al., 2020.

All DPD models were simulated in a $395.093 \times 395.093 \times 395.093 \text{ \AA}$ box, which was filled with 500,000 beads in total. The size of the simulation box was calculated using the assumed simulation density number, the total number of beads and the base unit for length as described by Pieczywek, Płaziński et al., 2020 (see also Supplementary Information). Solutions at the three different concentrations of GalA were simulated: 0.1 M (3920 GalA beads), 0.3 M (11730 GalA beads) and 0.5 M (19600 GalA beads). The concentrations were chosen to provide quantitatively representative systems, that could be relatively easily discussed with respect to the results available in literature and allow to observe the self-assembly mechanism in reasonable computation time. For each concentration the three types of homogalacturonan structures were simulated with differing chain lengths - chains with 10, 35 and 60 GlcA units. To test the effect of low and high pH, as well as pH $\sim pK_a$, each homogalacturonan chain was simulated in the three variations: a chain with all of the carboxyl groups being ionized, a chain with all of the carboxyl groups being protonated and a chain with half of the GalA units being protonated and half deprotonated (in a random order), respectively. Polysaccharides were initially generated as linear chains randomly located and oriented in the simulation box. In total, 27 simulation runs were carried out.

The time step of 0.001 in DPD units corresponded to 12.47 fs (based on time-scale calibration scheme described by Pieczywek, Płaziński et al., 2020). The total length of each simulation equal to ~ 120 ns was chosen based on the trial and error approach to track the time evolution of all simulated systems (both, quickly and slowly aggregating). All systems were initiated with 25,200 warm-up steps, and then were equilibrated for 10,080,000 steps. The simulation framework was implemented as a hand-written and multi-thread code using the C++ programming language (Pieczywek, Płaziński et al., 2020). The code architecture was optimized to perform computations using GPUs. This was achieved by including the OpenCL open-source library (Khronos Group, USA). The project was organized and compiled with the Microsoft Visual Studio Version 16.4.0 (Microsoft Corporation, USA).

2.4. Analysis of molecular trajectories

The self-aggregation abilities of simulated homogalacturonan chains and the structural features of the obtained aggregates were described by five parameters calculated from molecular trajectories – the percentage of aggregated chains, average group size, chain connectivity, the root mean square fluctuation of homogalacturonan chains (RMSF) and the radial distribution function of water molecules around pectic aggregates. The calculations of these parameters were based on prior definitions for group of molecules as well as the connection between two chains. In this study, two chains of homogalacturonan were considered to be connected when they had at least eight pairs of interacting galacturonic acid units. Two galacturonic acid units were considered to be an interacting pair, when the separation distance between them was smaller than the cut-off radius of the molecular interactions. Based on the abovementioned factors, a group of molecules was defined by at least five connected chains of homogalacturonan. Aggregates consisting of less than five chains were not counted as groups of molecules. The percentage of aggregated chains was defined as the percentage ratio of chains belonging to groups to the total number of HG chains in the system. The average group size was calculated as the percentage ratio of the average number of chains in groups to the total number of chains in the system. Chain connectivity was expressed as the ratio of the total number of connected chain pairs to the total number of homogalacturonan chains in the system. The root mean square fluctuations (RMSF) of the homogalacturonan chains was estimated based on the deviations of coordinates of the centres of mass of homogalacturonan residues with respect to the coordinates of the reference structure. The reference structure was a straight-line polysaccharide model of the same length. The radial distribution functions (RDF) expressed the probability

distribution of water molecules as a function of distance from the randomly selected coordinates from centres of nanofilaments or aggregates as the reference points.

3. Results and discussion

3.1. Association of *D*-galacturonic acid in aqueous solutions

3.1.1. GalA solutions at different concentrations and pH

The process of the self-association of molecules due to hydrogen bond formation is known to occur for carboxylic acids. Usually, dimerization (cyclic and linear dimer formation) is considered but the formation of higher associates in solution is also possible (Apelbast, 1991; Di Tomasso, 2013). In the case of GalA monohydrate, the results of X-ray studies showed that all $-\text{OH}$ groups of the molecule are donors, whereas oxygen atoms (except for O(1) and O(61)) are the acceptor atoms of hydrogen bonds. Moreover, the formation of hydrogen bonds between water and GalA molecules leads to the attainment of a hydrogen bonding network (Tang, Belton, Davies, & Hughes, 2001).

In the first stage of the experimental studies, the effect of GalA concentration in aqueous solution on the pH, electrophoretic mobility (EM), zeta potential (ZP) and measured hydrodynamic radius was investigated. The results are shown in Fig. 1.

The pH of the solutions decreased from 6.08 to 2.09 with the increase in GalA concentration from 10^{-5} to $2 \cdot 10^{-1}$ M. Simultaneously, a decrease from 0.97 to 0.04 in the calculated values of the dissociation degree was determined. A reduction in the dissociation degree to below 0.4 for the GalA concentrations lower than 10^{-3} M leads to a decrease in the absolute values of both EM and ZP. This may be connected with an increase in the ionic strength of the solution, a compaction of the electrical double layer around the molecules and a shortening of the distance between molecules which facilitated the association process due to hydrogen bond formation. For this range of GalA concentration, a decrease in the associate radius was observed, whereas for more diluted systems (GalA concentration $< 10^{-3}$ M) associate size increased with increasing GalA concentration. It is probable that in the low-concentration systems a small number of highly hydrated clusters of loosely bound molecules were present next to the ions. Their size increased up to some limit value, above that value a higher amount of more compact structures were formed.

3.1.2. The GalA solutions at different dissociation degree of molecules

Three concentrations of GalA (i.e. $3 \cdot 10^{-3}$, $3.3 \cdot 10^{-2}$ and $2 \cdot 10^{-1}$ M) were selected for further investigations of the influence of pH and the dissociation degree on associates formation. Due to KCl addition the electrolytic conductivity of all of the samples studied was at the level of 278 ± 29 mS/cm. The adjusted ionic strength allowed for the study of changes to EM and ZP in GalA solutions with respect to changes in pH (and therefore to the degree of protonation of the molecules) alone. The results are shown in Fig. 2.

For all GalA solutions the values of EM and ZP showed a similar decreasing trend with the increase in pH (Fig. 2a). At pH values between 0.35 and 3.51 the values of EM and ZP were positive, but falling close to zero at pH 3.51 for concentrations equal to $3.3 \cdot 10^{-3}$ M and $2 \cdot 10^{-1}$ M. At a concentration equal to $3.3 \cdot 10^{-2}$ M both parameters showed higher positive values compared to other solutions, but followed a similar decreasing trend. For a given concentration of GalA the decrease in pH value from 0.35 to 3.51 led to insignificant decrease in EM and ZP values. Further increase in pH significantly affected the EM and ZP. In alkaline conditions (pH 10.48), where the molecules should be totally dissociated, the values of EM and ZP for all tested concentrations were negative, varying from -0.211 to -0.487 $\mu\text{m cm/Vs}$ for EM and from -3.99 mV to -9.19 mV for ZP (independently from the GalA concentration).

Changes in the physicochemical properties corresponded very well with the measured median radii of the associates (Fig. 2b). With the exception of the $3.3 \cdot 10^{-2}$ M solution at pH 10.48 the DLS measurements

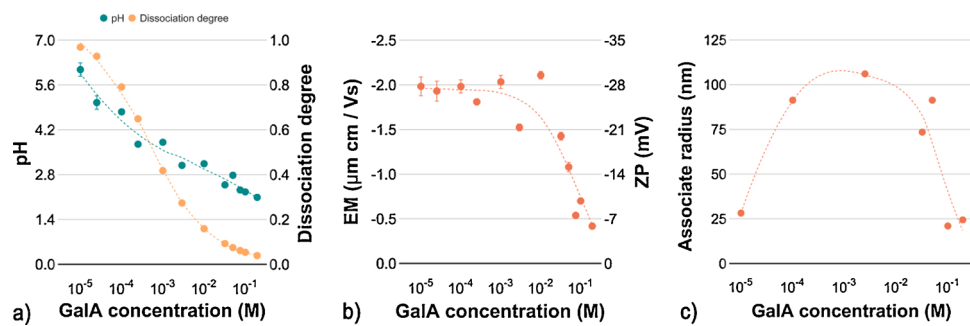


Fig. 1. Changes in a) pH and dissociation degree, b) electrophoretic mobility (EM) and zeta potential (ZP), and c) the median radius of associates with respect to the GalA concentration in aqueous solutions.

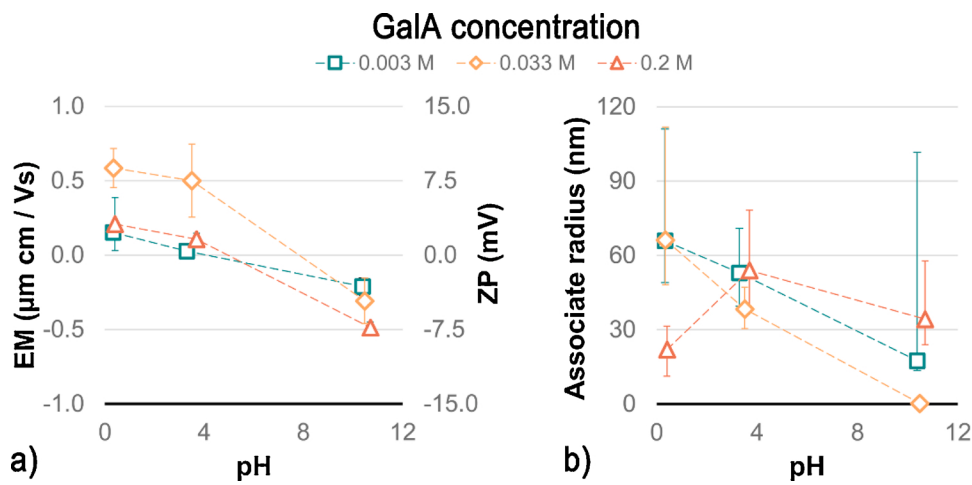


Fig. 2. Properties of GalA solutions under constant ionic strength: a) electrophoretic mobility (EM) and zeta potential (ZP) (bars indicate standard deviation), b) median radius of GalA associates at different pH and GalA concentrations (bars indicate lower (Q1) and upper quartile (Q3) respectively).

confirmed the presence of relatively large GalA associates in all tested samples. For concentrations of GalA equal to $3.3 \cdot 10^{-2}$ M and $2.0 \cdot 10^{-1}$ M an increase in the pH of the solution and therefore the dissociation degree of the GalA molecules resulted in a decrease of the radii of the associates. At both concentrations the largest associates were reported for pH 0.35 where the highest positive values of EM and ZP were reported, indicating a greater affinity of the GalA molecules to each other, as compared to the alkaline solutions. The decreasing size of the associates was a consequence of the higher number of negatively charged molecules and the higher degree of repulsion between negatively charged molecules in the GalA solution. For the $2.0 \cdot 10^{-1}$ M solution the median radii of the associates determined at pH 0.35 was the lowest among those obtained for the three GalA concentrations tested. This was consistent with the results presented in the previous section, which suggests the presence of more compact associates at high GalA concentrations. For the other pH values, the relationship between associate sizes and the concentration of GalA molecules was not so clear.

3.2. Homogalacturonan aggregation in water - DPD simulation

3.2.1. Pectin assemblies in aqueous solutions

The structure of polygalacturonic acid molecules was mapped into the DPD force field which allowed for an accurate representation of the molecules at the macroscopic scale. However, due to the simplified representation of the target system, detailed interpretations of molecular arrangements at the level of single polysaccharide chains should be performed with special care. Nevertheless, the simulations carried out in this study showed that pectin polysaccharide – homogalacturonan - had an intrinsic ability to form higher order structures in water. The

observed structures differed in shape and size with respect to homogalacturonan concentration, dissociation degree and chain length. Despite these differences two major patterns of aggregation were distinguished – ellipsoidal aggregates dispersed in water (Fig. 3 a,b) and a continuous three-dimensional network of polymer molecules (Fig. 3 d, e and Fig. 4).

The individual HG molecules maintained fairly linear shapes, showing a similarity with molecules from the homogalacturonan-rich diluted alkali soluble fraction of pectin observed using AFM (Pieczywek, Kozioł et al., 2020; Posé et al., 2012; Zdunek et al., 2014). However, the long straight rod-like structures (beyond 60 GalA units) previously visible in microscopy images (Pieczywek, Kozioł et al., 2020) were not reported in this study, suggesting additional factors affecting the shape of pectic molecules deposited on mica. As a result of the 1–4 glycosidic bond geometry, a characteristic helical arrangement of molecules was reported for complexes consisting of multiple chains (for dimers, trimers, etc., Fig. 3c). A similar helical arrangement of homogalacturonan chains was also observed in the case of calcium complexes during molecular dynamics simulations (Panczyk et al., 2018).

Ellipsoidal aggregates formed exclusively by short homogalacturonan chains (10 units of GalA, Fig. 4, Fig. 3 a,b) showed a high degree of resemblance to structures present in the water-soluble fraction of pectin (WSP). Normally, AFM images of WSP contain a significant amount of small round molecules which are believed to be loosely linked and depolymerized plant cell wall polysaccharides (Zdunek et al., 2014; Cybulska, Zdunek, & Kozioł, 2015; Gawowska, Cybulska, & Zdunek, 2018).

Although the process of forming higher order structures differs for homogalacturonan and for pure aqueous solutions of D-galacturonic

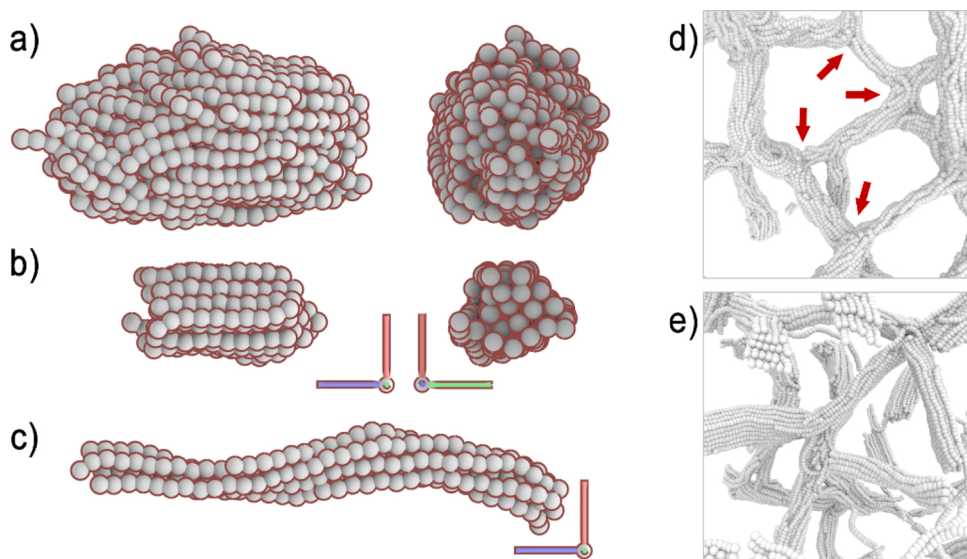


Fig. 3. Detailed images of the structures formed by homogalacturonan with respect to the length of chains: individual aggregates of short homogalacturonan chains (10 GalA units) at a dissociation degree equal to 0.0 (a) and 1.0 (b), helical twisting between relatively long homogalacturonan (35 GalA units) chains (c), network structures consisting of 35 GalA units, homogalacturonan chains with a dissociation degree equal to 0.0 (d) and 1.0 (e).

acid, the simulation results were qualitatively confirmed by the results of the experiment. Similarly to the case of the model system consisting of GalA monomers (Fig. 2b) deprotonation of the carboxyl groups resulted in a decrease in the size of the higher order structures (Fig. 3 a,b; Fig. 4; Fig. 5).

However, despite the qualitative similarity in trends, the size of the structures varied significantly between the experiment and the simulation results. For structures formed at a degree of dissociation close to zero, the radius of the biggest simulated aggregates was equal to ~5 nm, while experiments showed the presence of associates with a radius which was almost twelve times larger (Fig. 2b). The differences may be the result of a different mechanism of D-galacturonic acid associate formation and homogalacturonan aggregation, as well as the different time scales of the experiment (24 h of mixing) and simulation (120 ns of equilibration). Moreover, the size of the associate includes a hydration layer.

The protonation state of the carboxyl groups of GalA units changed not only the size but also affected the shapes of the simulated aggregates. For molecular assemblies of the protonated polysaccharides, individual chains were tightly packed and highly entangled. As a result, individual aggregates had ellipsoidal shapes with circular or ellipsoidal cross-sections along major and minor axes (Fig. 3a). Presumably due to a higher degree of chain stiffness and higher repulsion forces between the GalA units, deprotonated chains showed a parallel alignment with less helical twisting and entanglement between neighbouring polysaccharides (Fig. 3b). Similar differences between the shapes of the nanofilaments were also observed for network structures consisting of medium length chains (35 GalA units, Fig. 3 d and e). The structural differences disappeared for networks consisting of longer chains (60 GalA units), where the increased elasticity of the chains indicated by higher RMSF values (Fig. 6) allowed for more entanglement between the neighbouring polysaccharides.

3.2.2. Weak gel formation

The network structures obtained in simulations were believed to reflect the molecular structure of hydrated pectic gels. Since the simulation did not involve covalent bonding, the aggregation was driven by the simultaneous combination of inter-chain forces modified by hydrogen bonds and interactions between charged molecular chains and water molecules (Morris et al., 1979; Gidley, Morris, Murray, Powell, & Rees, 1980; Gilsenan et al., 2000; Pieczywek, Plaziński et al., 2020). The

resulting structures resembling aqueous gels consisted of three structural elements: junction zones where the polymer molecules were joined together, inter-junction segments and water pockets entrapped in a polymer network (Fig. 4). Junction zones are required for gelation and to provide a stable molecular structure for the polymer network (Oakenfull, 1991). However, some limitations in inter-chain association are also necessary to avoid the creation of insoluble aggregates and the collapse of the network structure. Unlike the “egg-box” model where Ca^{2+} binding of pectin requires 4–8 non-esterified GalA units (Braccini & Pérez, 2001), in this study junction zones were not restricted to specific molecular pairs and could be formed throughout the whole length of the chains. However, under specific conditions (mainly chain length and galacturonic acid concentration) stable networks were formed, indicating the presence of an important entropic factor that kept some sections of the chains apart. The observed stability of the structures was ensured by the entropic force resulting from the elasticity of the polysaccharide molecules. Among other pectic polysaccharides, homogalacturonan is known to exhibit considerable stiffness, thereby allowing it to adopt linear shapes when deposited on mica (Fishman, Cooke, Chau, Coffin, & Hotchkiss, 2007; Pose et al., 2012; Gawkowska et al., 2019; Pieczywek, Kozioł et al., 2020, 2020b). The shape of this polysaccharide is determined by the local stiffness resulting from the nature of the glycosidic bonds and the molecular structure of the basic sugar units. Molecular dynamics studies have shown that uronates such as galacturonan owe their high degree of conformational stability to 1–4 glycosidic linkages, which maintain their geometrical properties regardless of the degree of protonation and methylation of the carbohydrate residues (Panczyk et al., 2018). As a result, the relatively high degree of rigidity allows homogalacturonan to maintain a linear shape, thereby preventing its free ends from interacting. Reaching an energy minimum at which the formation of an aggregate from two chains takes place is only possible when the connected sections of molecules are arranged parallel to each other. At the same time, the chains are flexible enough to create a connection with more than one adjacent chain, this creates bridges between molecules, which forms the basis of the network.

Oakenfull & Scott (1984) described a similar mechanism in their studies of high-methoxyl pectin gelation under different temperatures and different cosolutes modifying hydrophobic interactions. They concluded that both hydrophobic interactions and hydrogen bonding are required for the formation of stable gel networks, with the free

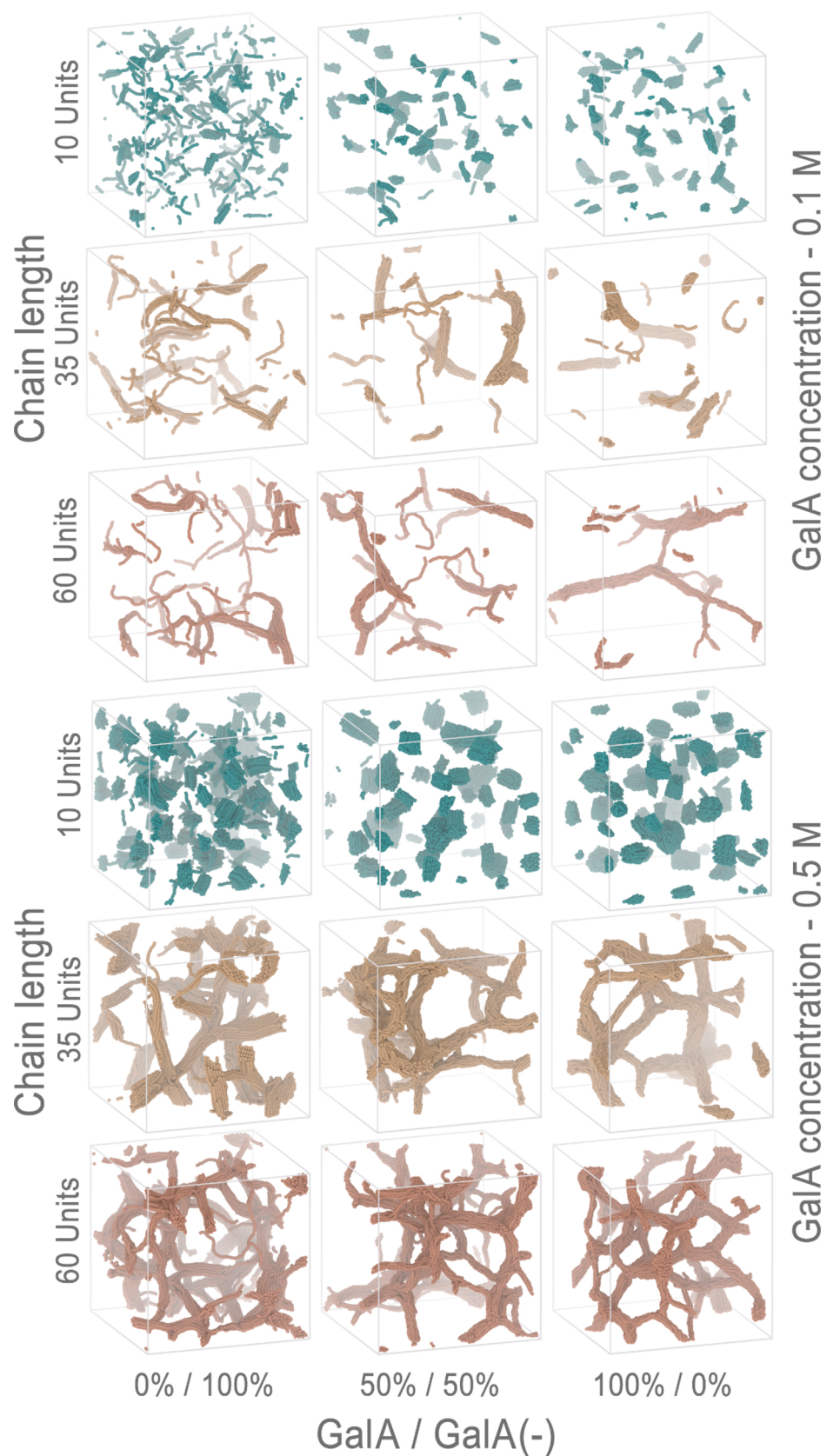


Fig. 4. Structures formed by homogalacturonan chains after 120 ns of equilibration with respect to chain lengths, concentration and the dissociation degree of GalA units.

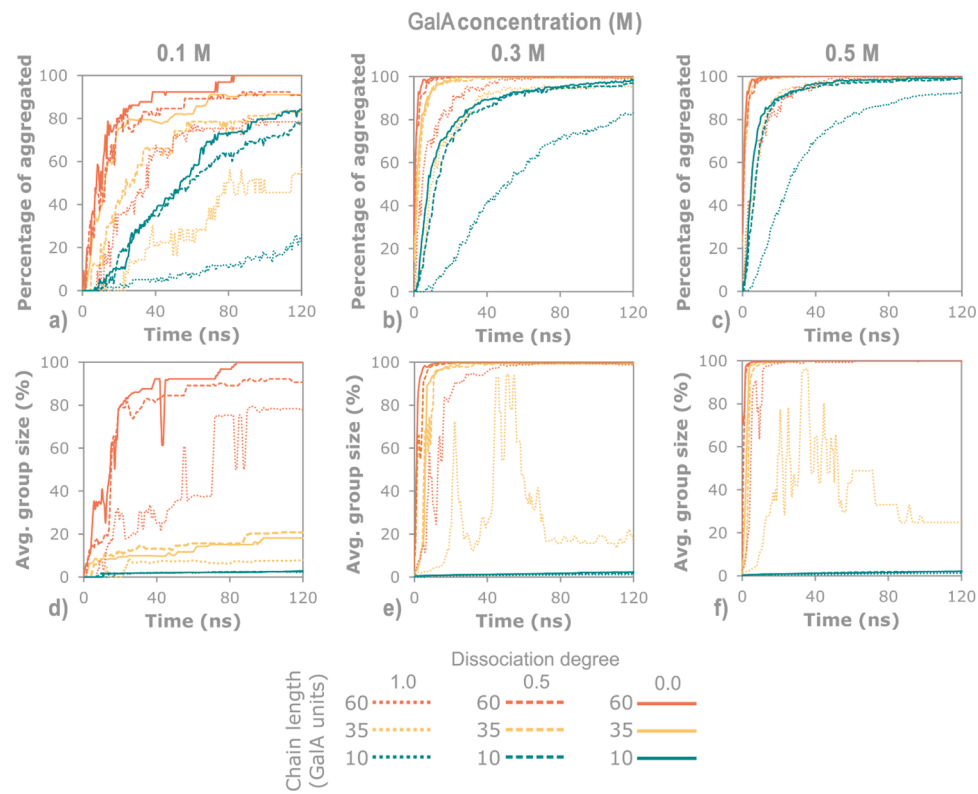


Fig. 5. Aggregation rate and structure connectivity expressed by the percentage of aggregated chains (a,b,c) and average group size (d,e,f) for different lengths of homogalacturonan chains and various concentrations and dissociation degrees of GalA units.

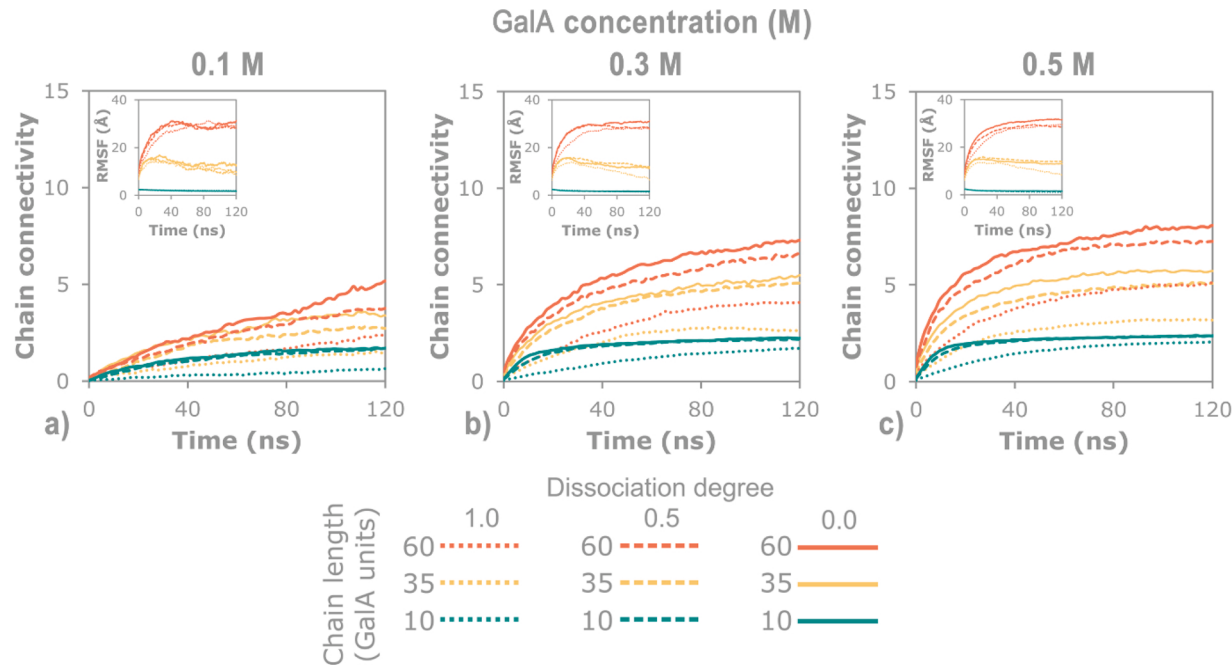


Fig. 6. The average connectivity of homogalacturonan chains (average number of neighbouring chains) for the different lengths of polysaccharide chain, at various concentrations and dissociation degrees of GalA units.

energy contribution of the formation of junctions by hydrophobic interactions being half that from hydrogen bonding.

The dynamic nature of the crosslinks complicates the physical description of the network properties, as the numbers and positions of non-covalent links can fluctuate with time (Ross-Murphy & Shatwell, 1993). Indeed, such behaviour was observed for simulated structures,

which despite establishing full network connectivity as indicated by the percentage of aggregated chains and average group size (Fig. 5 b, c, e, f, partially or fully protonated chains consisting of 35 or more GalA units at 0.3 M and 0.5 M after 40 ns), showed changes in chain connectivity (Fig. 6 b, c, from 40 ns to 120 ns) revealing ongoing continuous reorganization of the structure, driven by equilibration towards a current

energetic minimum. Weakly-bonded dynamic structures are prone to thermal fluctuations in the surrounding solvent and result in reduced abilities to transfer mechanical loads. Such properties are characteristic of weak gels. Weak gels are characterized by a linear viscoelasticity limited to relatively small strains (0.05), with the ability to flow without fracture, recover their structure and which exhibit the power law response during flow. In contrast, strong gels rupture and fail due to large deformation and do not return to their initial state without melting and resetting (Ross-Murphy & Shatwell, 1993). Weak gel-like properties that were indicated by oscillatory rheology experiments in the absence of a permanent network structure were reported for LM pectin at pH conditions close to or below the pK_a (Ström et al., 2014). Homogalacturonan-rich pectin was also classified as a pseudoplastic fluid (Mierczyńska, Cybulska, Pieczywek, & Zdunek, 2015; Mierczyńska, Cybulska, & Zdunek, 2017) which obeys the power law response during flow and exhibits shear thinning behaviour, where viscosity decreases with shear-rate.

In polymer solutions shear thinning is caused by the disentanglement of polymer chains during flow. Although flow experiments were not simulated in this study, it may be hypothesized that due to the presence of weakly-bonded junctions, the network structures (shown in Fig. 4) would gradually degrade when subjected to shear forces. The degree of network disentanglement and degradation depends on the rate of shearing, and presumably shows a decreased viscosity at higher shear-rates. At the same time, the intrinsic ability to self-aggregate would prevent its complete disentanglement and facilitate a complete restoration of the original structure of the gel after the cessation of the shear forces. Although further studies are required, it is believed that the described behaviour and properties of the presented coarse-grained models are sufficient to explain the macroscopic rheological properties of pectin and their ability to self-aggregate.

3.2.3. Dissociation degree of carboxyl groups

Crosslinking and gelation processes depend on many factors such as the pectin structure and its content, sugar and crosslinking agent concentration, temperature and pH (Gawkowska et al., 2018). In general, LM pectin is best known due to the formation of gel in the presence of divalent cations such as Ca^{2+} . This ability may be attributed to a stable dimeric “egg-box” structure which forms between two adjacent homogalacturonan chains in a two-fold conformation. The “egg-box” junction zone is formed by Ca^{2+} and at least 6–8 non-esterified GalA units from each chain (Braccini & Pérez, 2001; Panczyk et al., 2018). The strength of Ca^{2+} mediated gel increases with decreasing temperature and increasing calcium concentration (Clark, Evans, & Farrer, 1994; Lootens, Durand, Nicolai, Boulenguer, & Langendorff, 2003). Studies have reported such network structures at a broad range of pH from 3.5–9.0 (and corresponding dissociation degrees), with notably more compact structures being observed in basic conditions (Yang et al., 2018). This effect was attributed to the greater availability of deprotonated carboxyl groups which facilitated the formation of Ca^{2+} junction zones.

However, since the earliest studies of pectin gelation, other mechanisms were hypothesized whereby pectin of high and low ester content forms a gel without the involvement of divalent cations (Morris, Gidley, Murray, Powell and Rees, 1980). Such a mechanism at low pH and decreased water activity may be explained by the minimalization of intermolecular electrostatic repulsion which promotes chain-chain rather than chain-solvent interactions. Gilsenan et al. (2000) studied low-methoxyl pectin gelation in the absence of Ca^{2+} and at low pH. They reported that the protonation of carboxyl groups promoted conformational ordering and association leading to the formation of thermally reversible gels. They proposed the suppression of electrostatic repulsion and the hydrogen-bonding of carboxyl groups as two different mechanisms of LM pectin gelation. Similar results were reported by Ström et al. (2014), which showed that under pH conditions close to or below pK_a and in the absence of monovalent ions, low-methoxyl pectin exhibits weak-gel properties. The further addition of monovalent ions suggested

that the formation of structures exhibiting strong gel properties required both hydrogen bonding and monovalent ion involvement.

The equilibration of randomly dispersed HG chains was carried out in this study, the significant impact of the degree of dissociation of the carboxyl groups on the rate of aggregation of pectin was demonstrated. For completely deprotonated polysaccharides (Fig. 5 a, b, c - dotted lines) the percentage of aggregated chains increased at a much lower rate compared to the chains simulating low pH and $\text{pH} \sim pK_a$ (Fig. 4 a, b, c - solid and dashed lines). Structures simulating low pH and $\text{pH} \sim pK_a$ aggregated at a similar rate (Fig. 4 a - solid and dashed lines) and showed even fewer differences between each other at pectin concentrations higher than 0.1 M (Fig. 4 b, c - solid and dashed lines). This behaviour was a consequence of converting carboxyl groups from the ionized into the protonated form thereby suppressing electrostatic repulsion between the chains, which facilitated inter-molecular association and aggregation. Gilsenan et al. (2000) reported similar behaviour with slower kinetics of structure formation of LM pectin at pH 4.0 (above pK_a of GalA), where the degree of polysaccharide protonation was low. This was explained by the involvement of hydrogen bonding between the carboxyl groups on both chains which required the protonation of one of them. Since such a process was less likely to occur at high pH values, the resulting aggregation rate decreased, although higher order aggregates were still present. The higher affinity of simulated homogalacturonan chains with protonated carboxyl groups was also indicated by the higher inter-chain connectivity number (average number of neighbours per chain, Fig. 6 a, b, c) for chains of similar lengths and concentrations in water.

The GalA – H_2O radial distribution function profiles showed a higher average separation distance of GalA from water molecules for structures containing protonated carboxyl groups. For systems consisting of spherical aggregates (Fig. 7, chains with 10 GalA units) the higher separation distance corresponded to larger aggregates, while for network structures this indicated thicker nanofilaments (Fig. 7, chains consisting of more than 10 GalA units). Although differences between the RDF profiles were influenced by the concentration of GalA and the length of the chains, the general trend indicated the formation of larger aggregates with a decrease in the number of deprotonated molecules. Finally, the average size of the molecular aggregates consisting of interconnected HG chains (avg. group size) showed higher values for systems consisting of higher numbers of protonated molecules at concentrations equal to 0.1 M (Fig. 5d). A similar effect of pH on pectin aggregate size in aqueous solutions was reported by Sawayama, Kawabata, Nakahara, and Kamata (1988). In their study, light scattering measurements revealed an increase in the radius of the gyration of pectin aggregates when the pH of the solution was changed from 4 to 2. This effect was also confirmed by experimental results in the case of aqueous solutions of D-galacturonic acid (Fig. 1b). Results showed that the size of the associates decreased with each increase in the dissociation degree of the carboxyl groups (Fig. 2b). This was explained by the increase in the dissociation degree of the system and therefore, an increase in the pH, which resulted in a higher number of negatively charged GalA molecules (Fig. 2a). Hence, the higher degree of repulsion between negatively charged molecules in the GalA solution lead to smaller associations.

For chains consisting of 10 units of GalA, this effect was also observed at concentrations higher than 0.1 M (not visible in Fig. 5 d,e,f due to the applied scale). An increase in concentration (0.3 and 0.5 M) and the molecular weight of the HG chains (Fig. 5 e,f) partially suppressed the effect of the high repulsive forces between negatively charged molecules. For the longest simulated chains (60 GalA units) all of the systems equilibrated into networks consisting of all HG chains with a slightly slower aggregation rate for fully deprotonated GalA units (Fig. 5 d, e, f). For chains consisting of 35 GalA units, an alkaline environment simulated by fully deprotonated carboxyl groups resulted in an unstable system, unable to maintain network structures for the entire duration of the simulation (Fig. 5. e, f).

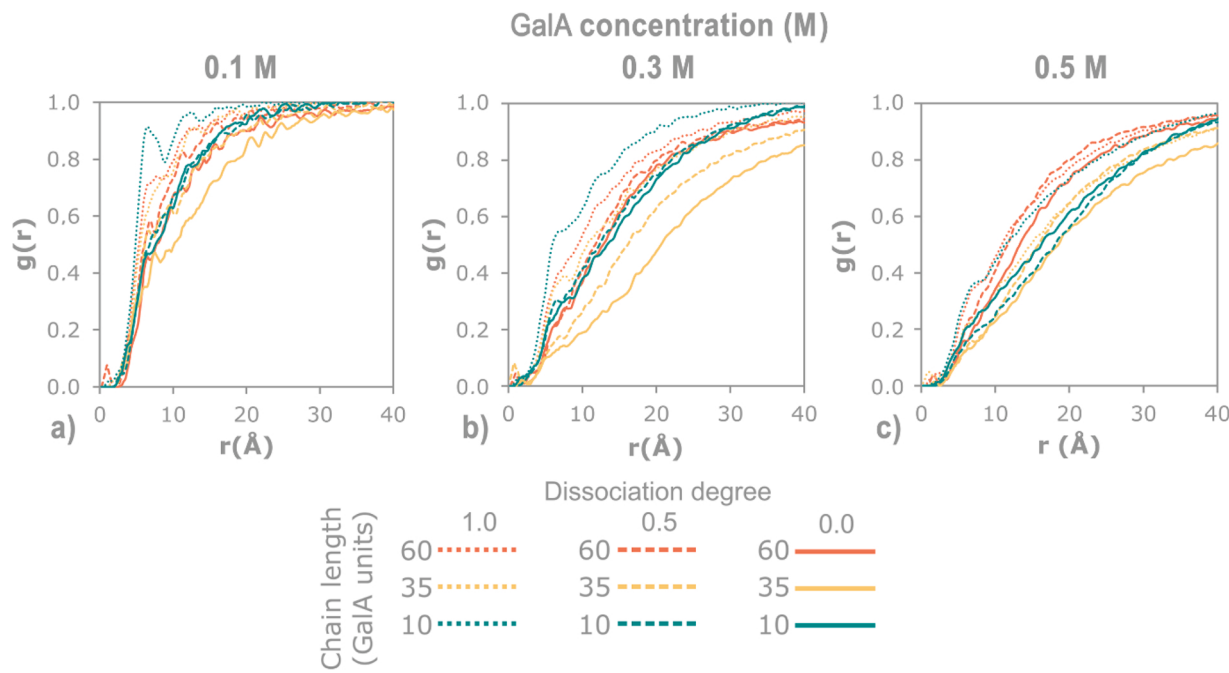


Fig. 7. The radial distribution functions showing the probability distribution of water molecules as a function of distance from the randomly selected coordinates from the centres of nanofilaments or aggregates, for different lengths of polysaccharide chain, at various concentrations and dissociation degrees of GalA units.

Although most of the research concerning pectin aggregation concerns their isolated forms, recent studies have indicated the important role of homogalacturonan charge in plant cell walls. Peaucelle et al. (2015) showed that molecule charge modifications through the de-methylesterification of cell-wall pectin triggered the selective wall loosening of *Arabidopsis* hypocotyl. The resulting mechanical asymmetry was considered to be a key factor required for the breakdown in growth symmetry.

The stiffening of HG due to the deprotonation of carboxyl groups was indicated by the RMSF values (Fig. 6), which, for similar lengths and concentrations of chains, were lower in the case of ionized molecules (a higher degree of stiffness means lower fluctuations in the shape of the chains). Chains consisting of 10 mers remained relatively stiff regardless of the charge/protonation state of the GalA units (sub-plots from Fig. 6).

3.2.4. Networking threshold

Although all of the tested conditions facilitated the aggregation of homogalacturonan chains into higher order structures, only one specific set of parameters enabled the formation of continuous three-dimensional networks. Such a set of parameters may be interpreted as the threshold below which a continuous network is unlikely to appear. Simulations showed that the length of the molecular chains had their highest impact on the networking ability of pectin in aqueous solutions. It was expected that due to the increased number of possible interaction sites, the increased ability to bend and the increased molecular weight, that longer molecules would provide more favourable conditions for network formation. Regardless of the concentration of GalA and the dissociation degree of carboxyl groups, chains consisting of less than 35 GalA units did not create a polymeric network. Despite the high percentage of aggregated chains (Fig. 5 a, b, c, green lines), the values of the average group size indicated the presence of a high number of small aggregates for chains consisting of 10 GalA (Fig. 5 d, e, f, green lines). Such objects may be observed in Fig. 4 (simulation cubes for chains consisting of 10 GalA) which show the higher order structures of homogalacturonan chains obtained due to self-aggregation after 120 ns of simulations. This observation is in line with the results of the gelation of high-methoxyl pectin as reported by Oakenfull and Scott (2006)). Their study of pectic gels showed that junction zones between two

adjacent segments of polysaccharide chains varied in length from 18 to 250 GalA units, and increased with the degree of methoxylation. The reported minimum size of the junction zone was approximately half the length of the 35 GalA chains simulated in this study, indicating the possibility of the presence of a structural threshold for network formation. In line with this assumption for concentrations of GalA equal to 0.3 and 0.5 M and chain lengths equal to or higher than 35 units, HG aggregated into fully-interconnected structures, consisting of all chains from the simulation box. An exception was reported for HG chains consisting of 35 GalA units at a degree of dissociation equal to 1.0. The length of chain close to the assumed threshold value with a high degree of dissociation of carboxyl groups prevented the formation of fully interconnected networks. Significant repulsive forces reflecting the interactions of deprotonated GalA molecules decreased the stability of the aggregates over time, this was indicated by the varying values of the average group size (Fig. 5 e, f - dotted yellow line). This set of parameter networks of high connectivity were only created for short periods of time, shortly after disintegrating into smaller structures.

4. Conclusions

The study showed that LM homogalacturonan aggregated into higher order structures in aqueous solutions regardless of the degree of dissociation of the carboxylic groups, the length of the chains and concentration. Depending on the properties and concentration of the polysaccharide, two major patterns of aggregation were observed for HG, namely ellipsoidal aggregates and a continuous three-dimensional network of polymer molecules. The study suggested the existence of a structural threshold for the formation of a spatial pectin network. For HG chains consisting of less than 35 GalA units, the formation of a stable gel structure was rather unlikely, and became impossible for chains with 10 GalA units. Longer chains enabled the formation of a fully connected network structure at low concentrations of pectin. Weakly interacting molecules formed networks with a stable but dynamically changing structure suggesting that its macroscopic properties may resemble those of weak gels. The equilibration of randomly dispersed HG chains carried out in this study, showed the considerable impact of the degree of dissociation of the carboxyl groups on the rate of self-assembly and

structural properties of pectin aggregates. The lower the degree of dissociation of the HG chains, the higher the rate of self-aggregation which was observed. The protonation of carboxyl groups facilitated the formation of larger aggregates or thicker nanofilaments depending on the type of final aggregates (individual aggregates or networks). This effect was also confirmed by experimental results in the case of water solutions of D-galacturonic acid, where the negative charge of the deprotonated molecules lead to the formation of smaller associates. The higher affinity of the simulated homogalacturonan chains with protonated carboxyl groups was also indicated by the higher degree of inter-chain connectivity. Simulations showed that at a constant degree of dissociation for the polysaccharide, an increase in the concentration and molecular weight of the HG chains facilitated the formation of self-assembled higher order structures, resulting in a higher rate of assembly and larger aggregates.

Funding

This study was supported by the National Science Centre, Poland (Project No. DEC-2015/17/B/NZ9/03589).

CRediT authorship contribution statement

Piotr Mariusz Pieczywek: Conceptualization, Formal analysis, Investigation, Methodology, Software, Visualization, Writing - original draft, Writing - review & editing. **Jolanta Cieśla:** Formal analysis, Investigation, Methodology, Writing - review & editing. **Wojciech Płaziński:** Investigation, Methodology, Writing - review & editing. **Artur Zdunek:** Funding acquisition, Writing - review & editing.

Declaration of Competing Interest

The authors declare no competing interests.

Acknowledgements

We would like to thank MSc Magdalena Koczańska, a Project DEC-2015/17/B/NZ9/03589 scholarship holder, for the preparation of GalA samples and performing part of measurements.

Appendix A. Supplementary data

Supplementary material related to this article can be found, in the online version, at doi:<https://doi.org/10.1016/j.carbpol.2020.117566>.

References

- Apelbast, A. (1991). Dimerization and continuous association including formation of cyclic dimers. *Canadian Journal of Chemistry*, 69, 638–647.
- Billy, L., Mehinagic, E., Royer, G., Renard, C. M. G. C., Arvisenet, G., Prost, C., et al. (2008). Relationship between texture and pectin composition of two apple cultivars during storage. *Postharvest Biology and Technology*, 47, 315–324.
- Bouton, S., Leboeuf, E., Mouille, G., Leydecker, M. T., Talbotec, J., Granier, F., et al. (2002). QUASIMODO1 encodes a putative membrane-bound glycosyltransferase required for normal pectin synthesis and cell adhesion in *Arabidopsis*. *The Plant Cell*, 14(10), 2577–2590.
- Braccini, I., & Pérez, S. (2001). Molecular basis of Ca^{2+} -Induced gelation in Alginates and pectins: The egg-box model revisited. *Biomacromolecules*, 2(4), 1089–1096.
- Broterman, S. E., & Schols, H. A. (2018). Interactions between pectin and cellulose in primary plant cell walls. *Carbohydrate Polymers*, 192, 263–272.
- Caffall, K. H., & Mohnen, D. (2009). The structure, function, and biosynthesis of plant cell wall pectic polysaccharides. *Carbohydrate Research*, 344(14), 1879–1900.
- Clark, A. H., Evans, K. T., & Farrer, D. B. (1994). Shear modulus–temperature meltdown profiles of gelatin and pectin gels. A cascade theory description. *International Journal of Biological Macromolecules*, 15, 125–130.
- Cosgrove, D. J., & Anderson, C. T. (2020). Plant cell growth: Do pectins drive lobe formation in *Arabidopsis* pavement cells? *Current Biology*, 30, R635–R662.
- Cros, S., Garnier, C., Axelos, M. A., Imbert, A., & Pérez, S. (1996). Solution conformations of pectin polysaccharides: Determination of chain characteristics by small angle neutron scattering, viscometry, and molecular modeling. *Biopolymers*, 39 (3), 339–352.
- Cybulska, J., Zdunek, A., & Kozioł, A. (2015). The self-assembled network and physiological degradation of pectins in carrot cell walls. *Food Hydrocolloids*, 43, 41–50.
- Delgado, A. V., Gonzales-Caballero, F., Hunter, R. J., Koopal, L. K., & Lyklema, J. (2007). Measurement and interpretation of electrokinetic phenomena. *Journal of Colloid and Interface Science*, 309, 194–224.
- Di Tomasso, D. (2013). The molecular self-association of carboxylic acids in solution: Testing the validity of the lily hypothesis using a quantum mechanical continuum solvation approach. *CrystEngComm*, 15, 6564–6577.
- Fishman, M., Cooke, P., Chau, H., Coffin, D., & Hotchkiss, A. (2007). Global structures of high methoxyl pectin from solution and in gels. *Biomacromolecules*, 8, 573–578.
- Gawkowska, D., Cybulska, J., & Zdunek, A. (2018). Structure-related gelling of pectins and linking with other natural compounds: A review. *Polymers*, 10(7), 762.
- Gawkowska, D., Cieśla, J., Zdunek, A., & Cybulska, J. (2019). Crosslinking of diluted alkali-soluble pectin from apple (*Malus domestica* fruit) in different acid-base conditions. *Food Hydrocolloids*, 92, 285–292.
- Gidley, M. J., Morris, E. R., Murray, E. J., Powell, D. A., & Rees, D. A. (1980). Evidence for two mechanisms of interchain association in calcium pectate gels. *International Journal of Biological Macromolecules*, 2(5), 332–334.
- Gilsenan, P., Richardson, R., & Morris, E. (2000). Thermally reversible acid-induced gelation of low-methoxy pectin. *Carbohydrate Polymers*, 41, 339–349.
- Grant, G. T., Morris, E. R., Rees, D. A., Smith, P. J. C., & Thom, D. (1973). Biological interactions between polysaccharides and divalent cations: The egg-box model. *FEBS Letters*, 32(1), 195–198.
- Groot, R. D., & Rabone, K. L. (2011). Mesoscopic simulation of cell membrane damage, morphology change and rupture by nonionic. *Surfactants. Biophys. J*, 81, 725–736.
- Haas, K. T., Wightman, R., Meyerowitz, E. M., & Peaucelle, A. (2020). Pectin homogalacturonan nanofilament expansion drives morphogenesis in plant epidermal cells. *Science*, 367(6481), 1003–1007.
- ISO 22412. (2017). *Particle size analysis – Dynamic light scattering (DLS)*. Geneva, Switzerland: International Organization for Standardization.
- Kohn, R., & Kováč, P. (1978). Dissociation constants of D-galacturonic and D-glucuronic acid and their O-methyl derivatives. *Chemicke Zvesti*, 32, 478–485.
- Li, Q., Xu, R., Fang, Q., Yuan, Y., Cao, J., & Jiang, W. (2020). Analyses of microstructure and cell wall polysaccharides of flesh tissues provide insights into cultivar difference in mealy patterns developed in apple fruit. *Food Chemistry*, 321, Article 126707.
- Lootens, D., Capel, F., Durand, D., Nicolai, T., Boulenguer, P., & Langendorff, V. (2003). Influence of pH, Ca concentration, temperature and amidation on the gelation of low methoxyl pectin. *Food Hydrocolloids*, 17(3), 237–244.
- Makshakova, O. N., Gorshkova, T. A., Mikshina, P. V., Zuev, Y. F., & Perez, S. (2017). Metrics of rhamnogalacturonan I with β (1→4)-linked galactan side chains and structural basis for its self-aggregation. *Carbohydrate Polymers*, 158, 93–101.
- Manunza, B., Deiana, S., Pintore, M., & Gessa, C. (1997a). A molecular dynamics investigation on the occurrence of helices in polygalacturonic acid. *Journal of Molecular Structure*, 419(1–3), 169–172.
- Manunza, B., Deiana, S., Pintore, M., & Gessa, C. (1997b). Molecular dynamics study of polygalacturonic acid chains in aqueous solution. *Carbohydrate Research*, 300(1), 85–88.
- Mayinger, F. (1994). *Optical measurements techniques and applications*. Berlin: Springer.
- Mierczynska, J., Cybulska, J., Pieczywek, P. M., & Zdunek, A. (2015). Effect of storage on rheology of water-soluble, chelate-soluble and diluted alkali-soluble pectin in carrot cell walls. *Food and Bioprocess Technology*, 8(1), 171–180.
- Mierczynska, J., Cybulska, J., & Zdunek, A. (2017). Rheological and chemical properties of pectin enriched fractions from different sources extracted with citric acid. *Carbohydrate Polymers*, 156, 443–451.
- Moeendarbary, E., Ng, T. Y., & Zangeneh, M. (2009). Dissipative particle dynamics: Introduction, methodology and complex fluid applications - A review. *International Journal of Applied Mechanics*, 1(4), 737–763.
- Mouille, G., Ralet, M. C., Cavelier, C., Eland, C., Effroy, D., Hématy, K., et al. (2007). Homogalacturonan synthesis in *Arabidopsis thaliana* requires a Golgi-localized protein with a putative methyltransferase domain. *The Plant Journal*, 50, 605–614.
- Noto, R., Martorana, V., Bulone, D., & San Biagio, B. L. (2005). Role of charges and solvent on the conformational properties of poly (galacturonic acid) chains: A molecular dynamics study. *Biomacromolecules*, 6, 2555–2562.
- Oakenfull, D. G. (1991). CHAPTER 5 - The chemistry of High-methoxyl pectins. In R. H. Walter (Ed.), *Food science and technology, the chemistry and technology of pectin* (pp. 87–108). Academic Press.
- Oakenfull, D., & Scott, A. (2006). Hydrophobic interaction in the gelation of high methoxyl pectins. *Journal of Food Science*, 49, 1093–1098.
- Palin, R., & Geitmann, A. (2012). The role of pectin in plant morphogenesis. *Bio-Systems*, 109, 397–402.
- Panczyk, K., Gaweda, K., Drach, M., & Plazinski, W. (2018). Extension of the GROMOS 56a6CARBO/CARBO-R force field for charged, protonated, and esterified uronates. *The Journal of Physical Chemistry B*, 122(14), 3696–3710.
- Paniagua, C., Santiago-Domenech, N., Kirby, A. R., Gunning, A. P., Morris, V. J., Quesada, M. A., et al. (2017). Structural changes in cell wall pectins during strawberry fruit development. *Plant Physiology and Biochemistry*, 118, Article 55e63.
- Peaucelle, A., Wightman, R., & Hofte, H. (2015). The control of growth symmetry breaking in the *Arabidopsis* hypocotyl. *Current Biology*, 25, 1746–1752.
- Pérez, S., Rodriguez-Carvajal, M. A., & Doco, T. (2003). A complex plant cell wall polysaccharide: Rhamnogalacturonan II. A structure in quest of a function. *Biochimie*, 85, 109–121.
- Persson, S., Caffall, K. H., Freshour, G., Hille, M. T., Bauer, S., Poindexter, P., et al. (2007). The *Arabidopsis* irregular xylem8 mutant is deficient in Glucuronoxylan and Homogalacturonan, which are essential for secondary cell wall integrity. *The Plant Cell*, 19, 237–255.

- Pieczywek, P. M., Kozioł, A., Plaziński, W., Cybulska, J., & Zdunek, A. (2020). Resolving the nanostructure of sodium carbonate extracted pectins (DASP) from apple cell walls with atomic force microscopy and molecular dynamics. *Food Hydrocolloids*, *104*, Article 105726.
- Pieczywek, P. M., Plaziński, W., & Zdunek, A. (2020). Dissipative particle dynamics model of homogalacturonan based on molecular dynamics simulations. *Scientific Reports*, *10*(1), Article 14691.
- Posé, S., Kirby, A. R., Mercado, J. A., Morris, V. J., & Quesada, M. A. (2012). Structural characterization of cell wall pectin fractions in ripe strawberry fruits using AFM. *Carbohydrate Polymers*, *88*, 882–890.
- Ralet, M. C., Crépeau, M. J., Lefebvre, J., Mouille, G., Höfte, H., & Thibault, J. F. (2008). Reduced number of homogalacturonan domains in pectins of an *Arabidopsis* mutant enhances the flexibility of the polymer. *Biomacromolecules*, *9*, 1454–1460.
- Ridley, B. L., O'Neill, M. A., & Mohnen, D. (2001). Pectins: Structure, biosynthesis, and oligogalacturonide-related signaling. *Phytochemistry*, *57*, 929–967.
- Ross-Murphy, S. B., & Shatwell, K. P. (1993). Polysaccharide strong and weak gels. *Biorheology*, *30*(3–4), 217–227.
- Round, A. N., Rigby, N. M., MacDougall, A. J., & Morris, V. J. (2010). A new view of pectin structure revealed by acid hydrolysis and atomic force microscopy. *Carbohydrate Research*, *345*, 487–497.
- Sawayama, S., Kawabata, A., Nakahara, H., & Kamata, T. (1988). A light scattering study on the effects of pH on pectin aggregation in aqueous solution. *Food Hydrocolloids*, *2*, 31–37.
- Ström, A., Schuster, E., & Goh, S. M. (2014). Rheological characterization of acid pectin samples in the absence and presence of monovalent ions. *Carbohydrate Polymers*, *113*, 336–343.
- Tang, H.-R., Belton, P. S., Davies, S. C., & Hughes, D. L. (2001). Solid state NMR and X-ray diffraction studies of α -D-galacturonic acid monohydrate. *Carbohydrate Research*, *330*, 391–399.
- Thibault, J.-F., & Ralet, M.-C. (2003). Physico-chemical properties of pectins in the cell walls and after extraction. In book: *Advances in Pectin and Pectinase Research*, 91–105.
- Wolf, S., Mouille, G., & Pelloux, J. (2009). Homogalacturonan methyl-esterification and plant development. *Molecular Plant*, *2*(5), 851–860.
- Yang, X., Nisar, T., Liang, D., Hou, Y., Sun, L., & Guo, Y. (2018). Low methoxyl pectin gelation under alkaline conditions and its rheological properties: Using NaOH as a pH regulator. *Food Hydrocolloids*, *79*, 560–571.
- Zdunek, A., Kozioł, A., Pieczywek, P. M., & Cybulska, J. (2014). Evaluation of the nanostructure of pectin, Hemicellulose and cellulose in the cell walls of pears of different texture and firmness. *Food and Bioprocess Technology*, *7*(12), 3525–3535.
- Zetasizer Nano User Manual. (2004). *Zetasizer nano user manual*. Malvern, UK: Malvern Instruments Ltd.